

Optical Buffer and Link Dimensioning to Support Video Traffic with Scaling Characteristics

E. Santos Jr. and R. F. Coelho

Abstract—The performance of optical switched networks (OSN) to support video traffic with scaling characteristics and different QoS requirements is studied in this paper. The $M/G/\infty$ and fBm processes are considered to model the video input traffic. These processes are examined in terms of its video traffic scaling (H), heavy-tail distribution (HTD) and autocorrelation (ACF) characterization. A new frame-to-burst (FTB) assembly is proposed to enable the optical edge-switches to deal with video traffic. We demonstrate that video traffic tail distribution is more critical to the optical switch dimensioning and thus OSN performance than the scaling characteristics.

Index Terms—Optical switched networks, video traffic modeling, Hurst or scaling estimation

I. INTRODUCTION

THE progress of full-optical networks not only enables new switching technologies but also reduces telecommunication transmission costs. These networking achievements associated with video coding improvements such as digital storage and interactive systems capacity gave impulse to the bandwidth demanding video services. Hence, video is a key traffic to be supported by the future optical switched networks.

The transport of multitraffic with quality-of-service (QoS) guarantee is a traffic engineering challenge since the deployment of ATM high-speed networks. The recent possibility of bringing the switching function to the optical domain led to new challenges to this research area.

In this paper we study the performance of optical switched networks to support video traffic with scaling or time-dependence characteristics and different QoS requirements. Video traffic has an inherent scaling invariance due to its encoding process. The scaling degree is here defined by the Hurst (H) parameter [10]. The analysis presented in this work concerns two major parts. In the first one, we examined the performance of the *restricted* $M/G/\infty$ [12] and the *non-restricted* fBm (fractional Brownian motion) [15] models to represent the video input processes. The $M/G/\infty$ and fBm performance were compared in terms of the models video traffic scaling (H), heavy-tail distribution (HTD) and autocorrelation (ACF) characterization. The terms *restricted* or *non-restricted* are related to the models ability to represent the video scaling characteristics range or second-order statistics. These terms also refer to the scaling representation duration. In the second part of the analysis, the optical switched network (OSN) based on burst-edge-switch architecture (OBS) (Fig. 1) is evaluated, i.e., the switching queueing behavior when fed by the $M/G/\infty$ and the fBm video input processes.

E. Santos Jr. and R. F. Coelho, Instituto Militar de Engenharia, Rio de Janeiro, Brasil, E-mail:coelho@ime.eb.br. This work was supported by FAPERJ under grant number E-26/171.374/01.

A new frame-to-burst (FTB) assembly is proposed to the burst-edge-switch to deal with video traffic. The performance of OBS has been widely studied for IP data burst traffic optical networks. These studies are basically centered on the packet-to-burst assembly function [6], [24], [27] or wavelength reservation protocol [7]. We demonstrate that the video traffic distribution is a critical point to the optical switch performance. We also show that the video scaling were not affected by the large buffer sizes and different edge delay. For the experiments we use several video sequences from different encoding processes. The results derived from this study lead to the optical buffer switch and link rate dimensioning considering different video QoS requirements.

The reminder of the paper is organized as follows. In Section II we present the optical switched network architecture examined in this work. Section III describes the $M/G/\infty$ and fBm processes that are evaluated to model the video traffic sources. Section IV presents the $M/G/\infty$ and fBm performance results. The edge-switch performance analysis and optical link dimensioning results are present and discussed in Section V. Finally, Section VI is devoted to the conclusion of this work.

II. THE OPTICAL SWITCHED NETWORK ARCHITECTURE

Packet [8], [5], [20], [9] and burst [26], [19], [7] switching techniques were studied to achieve the best optical switching architecture for WDM (wavelength division multiplexing) networks. A generic optical packet switching architecture is concerned of tunable wavelength converters (λC), optical buffering carried by fiber delay lines (FDL) and optical gates. The well known KEOPS (KEYs of Optical Packet Switching) architecture [8] was a promising solution to provide packet switching in a transparent full-optical network.

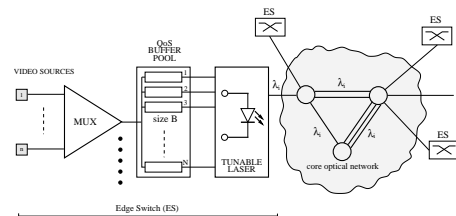


Fig. 1. A generic Edge-Route OBS network architecture

The needs of wavelength converters in all network switches leads to a very expensive network design project. The FDLs were then implemented to reduce the number of switches with λC but they increase the network jitter and routing complexity.

The optical burst switching (OBS) [26], [19] was then proposed as a solution to avoid the limitations and problems of the other switching possibilities. The electronic burst switching (EBS) also known as fast-circuit switching were widely investigated for ATM networks. Boyer [3] proposed a fast-reservation protocol¹ (FRP) with delayed (FRP-DT) and immediate (FRP-IT) transmission to provide burst data transport with bandwidth release after the burst deliverance.

In an optical switched network with OBS architecture the traffic processing is done at the network edging. The objective is to avoid the same impairments of the optical packet switching fabrics. Thus, the control and data information are treated separately by edge-switch-routers. The edge processing is responsible for the burst-assembly and wavelength reservation functions. This solution remove the complexity from the optical core network. The information-to-burst assembly is indeed a traffic shaping (TS) function. This TS is applied even to original data-burst (ON-OFF) sources to achieve lower optical transmission cost. The wavelength reservation is done during the burst-assembly period in an one or two-way reservation procedure. Several wavelength reservation protocols similar to the FRP approach such as TAG (Tell-and-Go), RFD (Reserve-a-Fixed-Duration) and JET [27] (Just-Enough-Time) were investigated for OBS networks.

In [7] the authors proposed a dynamic wavelength reservation for an OBS architecture. They also introduce a wavelength reuse factor (RUF) that enables the unused wavelength to be assigned to another edge-router.

The performance of the OBS has been widely studied for IP data burst traffic. In this paper we examine the performance of OBS networks to support video services with scaling characteristics and different QoS requirements (see Fig. 1). Our analysis present a complete OBS evaluation including different input processes, scaling degree, buffer sizes, edge delay, optical link rate and packet-loss requirements. A new frame-to-burst assembly is also proposed to enable the burst-switch to deal with video traffic.

III. THE SCALING VIDEO TRAFFIC MODELING

The main drawback of the traffic engineering researches concerns the lack of accurate source and network traffic models. An accurate traffic model should represent the first and second-order statistics. Besides, it should be tractable in terms of queueing theory. In our analysis we examined the performance of the $M/G/\infty$ point process and fBm models to represent different input first and second-order video statistics. The fBm and $M/G/\infty$ are considered monofractals since these processes generate sample paths with constant scaling degree. In [21] several measurements showed that the network traffic can present scaling variability after a period of time greater than four hours, i.e., the scaling is only considered as constant or monofractal during an interval less than four hours. In [1] a multifractal version of the fBm process is introduced where H is defined as function of the Hölder regularity ($H = h(t)$; $0 < h(t) < 1$). Multifractal processes

can be interesting to model network traffic due to its scaling variability. However, it needs more investigation and accuracy to deal with queueing performance. The optical edge-switch performance is further investigated to support this two input processes. A stochastic process $X(t)$ can be classified by its scaling degree as positive or long-range dependent (LRD) ($H > \frac{1}{2}$), short-range dependent (SRD) ($H = \frac{1}{2}$) or negative or anti-persistent ($H < \frac{1}{2}$). Some authors denote all processes with $H \leq \frac{1}{2}$ as SRD. In the literature it is possible to find LRD processes defined as self-similar. However, a process can only be considered self-similar if its statistical characteristics, i.e., marginal distribution and scaling degree, holds for any time scale. By definition $M/G/\infty$ represents positive scaling degree for a certain period of time. This restricted time shall be however enough to investigate the impact of the video traffic dependence on the optical switch queueing performance measures. The fBm is here defined as the non-restricted scaling model since it can represent the entire time-dependence range, i.e., $0 < H < 1$. The fBm and $M/G/\infty$ are defined as monofractals since they generate sample paths with constant scaling degree. For the analysis, we examined several video traces with different monofractal scaling degrees.

A. $M/G/\infty$

The $M/G/\infty$ [12] input or source process is represented by an infinite server with G distribution service time ($P[Z > t]$) fed by a Poisson process with λ mean arrival rate, i.e., the input process is defined by λ and the G distribution. Hence, we have that

$$P[Z > t] = \frac{\gamma(t) - \gamma(t+1)}{1 - \gamma(1)}, \quad t = 0, 1, \dots \quad (1)$$

where $\gamma(t)$ is the autocorrelation function of the $Z(t)$ process. The $M/G/\infty$ autocorrelation is defined by $\Gamma(t) = \delta^2 \gamma_H(t)$, $h = 0, 1, \dots$ where $H = 1 - \beta/2$ and $\beta(0 < \beta < 1)$ and δ^2 are constants. To achieve the positive scaling representation the $M/G/\infty$ input process ($Z_H(t)$) must have a decreasing and integer-convex ACF ($\gamma_H(t)$) with $\gamma_H(0) = 1$. Therefore,

$$\gamma_H(t) \sim H(2H - 1)t^{2H-2}, \quad t \rightarrow \infty \quad (2)$$

To find the G service time distribution and considering the previous ACF definition we must have

$$P[Z_H > z] = \frac{|z + 2|^{2H} - 3|z + 1|^{2H} + 3|z|^{2H} - |z - 1|^{2H}}{4(1 - 2^{2H-2})}, \quad z = 1, 2, \dots \quad (3)$$

The $M/G/\infty$ also considers that the video traces ACF ($\rho(k)$) is

$$\rho(k) = e^{-\beta\sqrt{k}}, \quad k = 0, 1, 2, \dots \quad (4)$$

The β parameter is obtained from the real video traces. The G distribution is then related to video trace ACF by the expression

$$P[Z = k] = \frac{\rho(k-1) - 2\rho(k) + \rho(k+1)}{1 - \rho(1)} \quad (5)$$

Finally, the $M/G/\infty$ samples are generated by a Poisson to hybrid Gamma (F_G)/Pareto (F_P) distribution transformation

¹The ITU FRP is described in the ITU-T I.371 Recommendation *Traffic Control and Congestion Control in B-ISDN*, 1995.

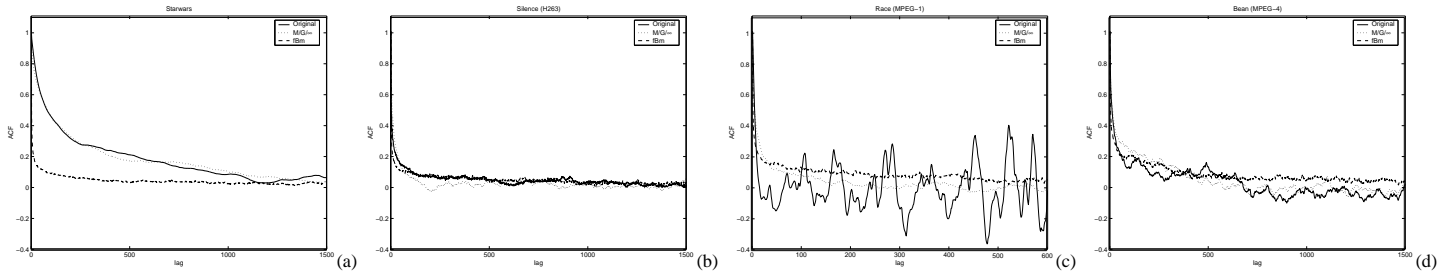


Fig. 2. ACF for (a) StarWars, (b) Silence, (c) Race and (d) Bean Sequences.

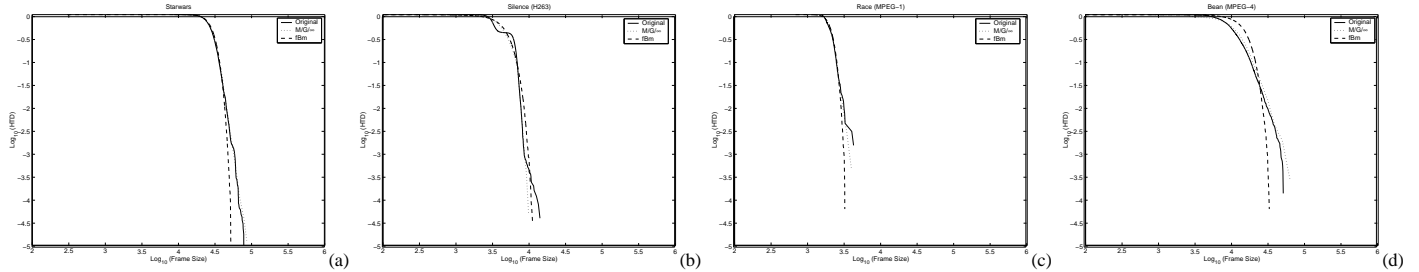


Fig. 3. HTD for (a) StarWars, (b) Silence, (c) Race and (d) Bean sequences.

(F_{PGP}) to keep the ACF (cf. Eq. 4) obtained from the video traces, i.e., for some $x^* > 0$ $F_{PGP} = \begin{cases} F_G(x) & \mathbf{x} \leq x^* \\ F_P(x) & \mathbf{x} > x^* \end{cases}$.

As previously mentioned, the $M/G/\infty$ model has a restricted scaling representation in terms of its range and duration. Its main advantage concerns its markovian properties and thus leading to tractable queuing analysis.

B. fractional Brownian motion

The fractional Brownian motion (fBm) [15] is a gaussian stochastic process ($X_H(t)$) indexed in \mathfrak{R} with zero mean and continuous sample path (null at origin). The fBm is known as the unique gaussian H-sssi, i.e., self-similar with self-similarity parameter and stationary increments. The variance of the independent increments is proportional to its time interval accordingly to the expression

$$\text{Var}[X(t_2) - X(t_1)] \propto |t_2 - t_1|^{2H}, \quad (6)$$

for $0 \leq t_1 \leq t_2$. It can be proven [15] that the fBm is a stationary and self-similar process with parameter H , i.e., its statistical characteristics holds for any time scale. Thus, for any τ and $r > 0$, we have

$$[X_H(t+r\tau) - X_H(t)] \stackrel{d}{\approx} r^{-H} [X_H(t+r\tau) - X_H(t)] \quad (7)$$

where r is the process scaling factor. Since $X_H(t)$ is gaussian, it is completely characterized by its mean (null) and its ACF which is given by

$$\rho(k) = \frac{1}{2} \sigma^2 [(k+1)^{2H} - 2k^{2H} + (k-1)^{2H}]. \quad (8)$$

Norris [17] proposed a discretization procedure that enables a fBm model to generate an input process ($A(t)$) with scaling characteristics and non-zero mean and a variance. Denoting

$A(t)$ as the number of received packets by a multiplexer up to time t , we have

$$A(t) = mt + \sqrt{am} X_H(t), \quad (9)$$

where m is the mean rate of the arrival process and $a = \text{Var}[A(t)]/t^2$ is a variance coefficient.

For the simulation experiments the fBm sample paths were generated by the simple and well known *Random Midpoint Displacement* [2] algorithm. The fBm samples generation depends only on m , σ and H parameters. However, the G distribution fitting procedure of the $M/G/\infty$ model presented in section III-A leads to a complex sample generation.

IV. THE VIDEO TRAFFIC PERFORMANCE MODELING RESULTS

This section presents the $M/G/\infty$ and fBm performance to represent the scaling, heavy-tail distribution and autocorrelation of a video input process. The optical switched network performance are further evaluated under these stochastic processes. Four encoded video sequences [25] *StarWars* (JPEG), *Silence of the Lambs* (*Silence*) (H.263), *Mr. Bean* (MPEG-4) and *Race* (MPEG-1) were considered in the experiments.

TABLE I
VIDEO SEQUENCES PARAMETERS.

Sequence	m (kbits/s)	σ (kbits/s)	$\bar{H}(R/S)$	$\bar{H}(AV)$
<i>StarWars</i> (JPEG)	5335.8	1200.8	0.830	0.828
<i>Silence</i> (H.263)	891.6	344.09	0.822	0.820
<i>Bean</i> (MPEG-4)	183.92	179.0	0.817	0.822
<i>Race</i> (MPEG-1)	1804.8	537.79	0.870	0.888

A. The Scaling Representation Results

For the scaling representation evaluation we use the Rescaled/Statistics (R/S) [10] and AV-Wavelet [22] estimators.

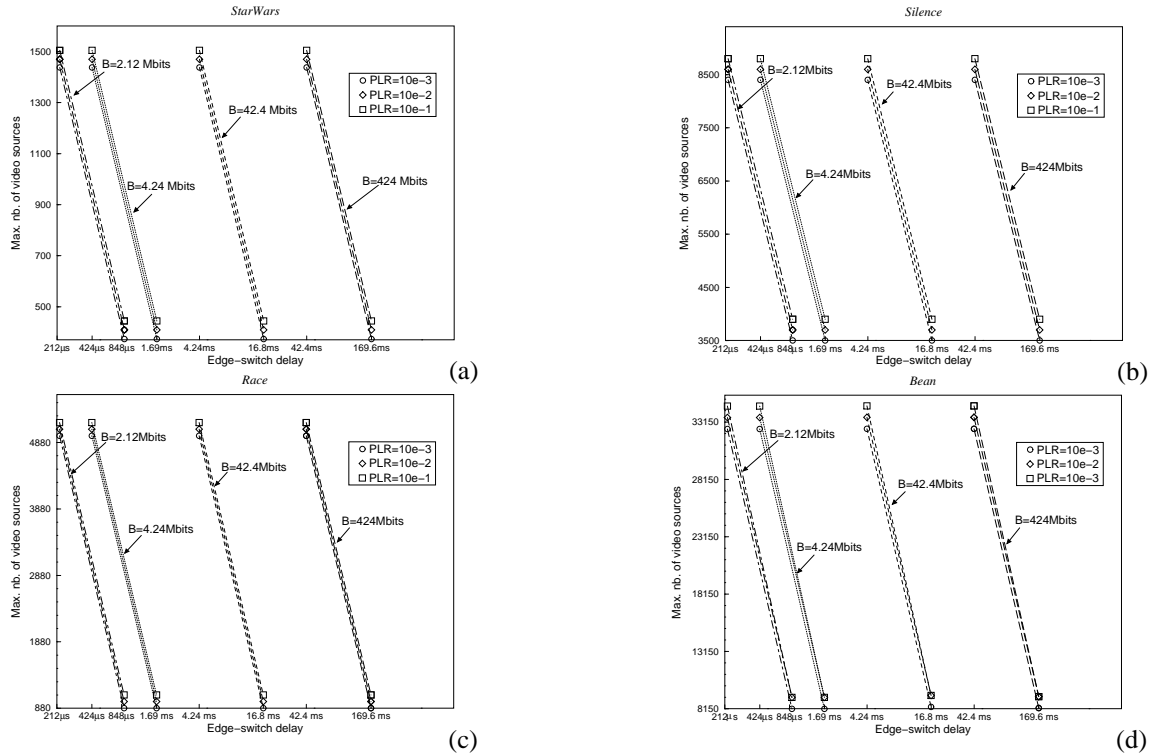


Fig. 4. The Edge-Switch Performance Results- $M/G/\infty$ (a) StarWars, (b) Silence, (c) Race and (d) Bean sequences.

These estimation methods presented quite similar results for each of the video sequences. The AV-Wavelet presented lower complexity due to its faster estimation algorithms. Several estimation results and discussion concerning the video traffic scaling is presented in [18].

Table I illustrates the estimated Hurst (\hat{H}) parameters obtained from the real video traces. The video sequences scaling degree were also estimated after the edge-buffering and the results are shown in section V-B

As we note all the sequences present LRD characteristics. We chose these LRD sequences in order to examine the optical edge-switch under worst traffic conditions. Sources with $H \leq 1/2$, presenting the anti-persistence effect [4] [14], are strongly centered around its mean rate and thus we expect better queuing performance compared to LRD sources. Moreover, by definition the $M/G/\infty$ model can only represent positive scaling.

B. ACF Results

Fig. 2 illustrates the ACF curves obtained from the original video traces and for the $M/G/\infty$ and fBm models. The $M/G/\infty$ presented better ACF fitting results compared to the fBm for the video sequences with subexponential ACF (e.g. *StarWars*). However, this was not the case for the *Race* sequence. The best ACF fitting considering both models was achieved for the *Silence* (Fig 2.b) sequence.

C. Heavy-Tail Distribution Results

By definition we say that a random variable X has a heavy-tail distribution if

$$P(X > x) \cong cx^{-\alpha}, \quad x \rightarrow \infty. \quad (10)$$

where $0 < \alpha < 2$ is the shape parameter and c is a positive constant [13]. The Pareto distribution is an important HTD since it well fits the heavy-tail distribution of the LRD processes. Note that the $M/G/\infty$ model uses the Poisson to Gamma/Pareto transformation (F_{PGP}) to fit the real video sequences ACF and HTD. The HTD results for the original video sequences and the models are depicted in Fig. 3.

The $M/G/\infty$ and fBm tail distributions were very close for the *Race* (cf. Fig. 3.c) sequence. For the *Bean* sequence however the fBm HTD were quite different from original video trace.

V. THE EDGE-SWITCH PERFORMANCE ANALYSIS AND OPTICAL LINK DIMENSIONING

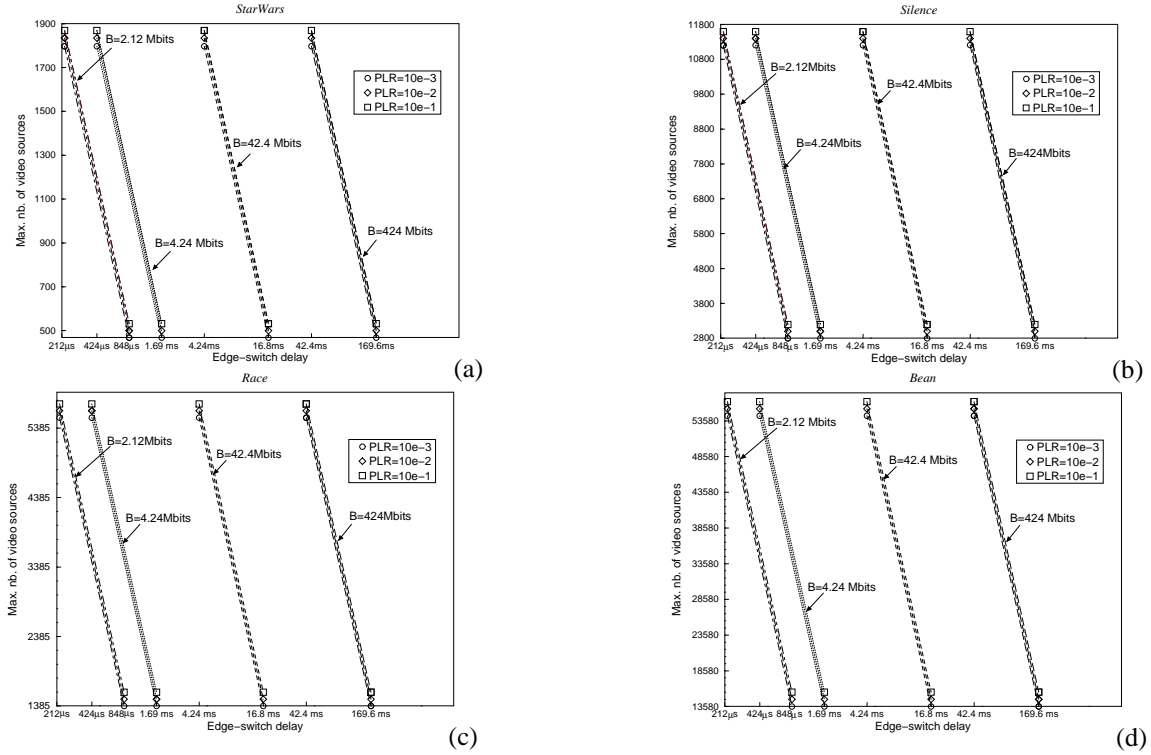
We propose a new frame-to-burst (FTB) assembly for the optical edge-switch. In the FTB function the encoded bits collected from video frames are gathered to complete a burst. This assembly function shall however keep the video delay QoS requirements.

For the QoS buffer-pool queues dimensioning we considered different burst sizes (B), optical link rates (C) and edge-burst-processing delay (t_{ebp}).

TABLE II
EDGE-BURST-PROCESSING DELAY.

Burst size (B) in bits	$C = 10\text{Gbits/s}$	$C = 2.5\text{Gbits/s}$
2.12M	212 μs	848 μs
4.24M	424 μs	1.696 ms
42M	4.24 ms	16.8 ms
424M	42.4 ms	169.6 ms

Table II illustrates the t_{ebp} values as function of the different optical burst sizes and link rates. The switch queuing behavior


 Fig. 5. The Edge-Switch Performance Results- fBm (a) StarWars, (b) Silence, (c) Race and (d) Bean sequences.

fed by the $M/G/\infty$ and fBm video processes are then evaluated considering these parameters.

The queueing behavior and the respective QoS are here represented by the maximum number of multiplexed video sources (n_{max}), the packet loss ratio (PLR) and the edge-processing delay. Simulations were run considering the $M/G/\infty$ and fBm processes and were compared to theoretical results. The buffer dimensioning (the equations considering the scaling input processes are presented in Section V-B.

A. Edge-Switch Buffer and link dimensioning

Consider $A(t)$ as a fBm process, defined in Eq. 9 with parameters m , a and H ; a queue system with deterministic service C (optical link rate) and an infinite buffer queue Q . The buffer queue behavior is thus a stochastic process $Q(t)$ defined as

$$Q(t) = \sup_{s \leq t} (A(s) - C(t - s)), \quad t \in (-\infty, \infty). \quad (11)$$

If $\epsilon \in \mathbb{P}(Q \leq B)$ is the probability that a buffer of size Q becomes larger than a certain limit B , it follows that the required bandwidth of an aggregate flow of n video flows $C_A(n)$ is

$$C_A(n) = \kappa(H) \left(\sqrt{-2 \ln \epsilon} \right)^{\frac{1}{H}} B^{\frac{H-1}{H}} (nma)^{\frac{1}{H}}, \quad (12)$$

where $\kappa(H) = H^H (1-H)^{1-H}$. Thus, the maximum number of video connections (n_{max}) that can be multiplexed in an optical link with capacity C considering an edge-switch queueing buffer size (B) is determine by

$$n_{max} m \left(\sqrt{-2 \ln \epsilon} \right)^{\frac{1}{H}} B^{\frac{H-1}{H}} (n_{max} ma)^{\frac{1}{H}} \leq C. \quad (13)$$

For a detailed description of these definitions and formulations the reader should refer to [11] and [17].

TABLE III
MAX. NUMBER OF MULTIPLEXED VIDEO SOURCES IN 10GBITS/S AND 2.5GBITS/S AND $PLR=10^{-x}$, $x = 3, 2, 1$

B (in bits)	2.12M	4.24M	42M	424M
StarWars- $theo/fBm$	1798-468	1798-468	1799-468	1797-468
StarWars- $M/G/\infty$	1438-374	1439-374	1439-375	1439-378
Silence- $theo/fBm$	11204-2803	11206-2803	11211-2803	11212-2803
Silence- $M/G/\infty$	8403-2102	8406-2102	8410-2102	8408-2102
Bean- $theo/fBm$	54272-13586	54300-13588	54280-13589	54278-13586
Bean- $M/G/\infty$	32563-8152	32563-8153	32580-8222	32580-8230
Race- $theo/fBm$	5535-1385	5537-1385	5536-1385	5537-1385
Race- $M/G/\infty$	4981-883	4982-883	4981-882	4981-884

B. The Edge-Switch Performance Results

We begin this section by showing the scaling estimation results examined after the FTB assembly (see Table IV). As expected, the H values did not present significant changings even for larger buffer sizes ($B = 424Mbits$), i.e., the scaling is not affected by the assembly function. This similar behavior were found in ATM networks performance studies [16].

TABLE IV
VIDEO SEQUENCES SCALING AFTER EDGE-BUFFERING.

Sequence	$\bar{H}(AV)$			
	B=2.12Mbits	4.24Mbits	42Mbits	424Mbits
StarWars	0.896	0.898	0.892	0.892
Silence	0.822	0.813	0.822	0.812
Bean	0.844	0.853	0.845	0.848
Race	0.862	0.860	0.860	0.862

The edge-switch simulation results for both models were compared to the theoretical values obtained from the equations presented in section V-A. For these experiments we considered the parameters setting illustrated in Table II. The video information loss is represented by $PLR = 10^{-x} \approx FQ > B$ where $x = 3, 2, 1$ only to reduce the simulation run-time.

In OBS networks these packet losses are due to the frame-to-burst assembly but the information is not necessarily lost since the data can be sent to one of the N queues present in the QoS buffer-pool.

The theoretical and simulation curves for the $M/G/\infty$ and fBm input processes are reported on Figs. 4 and 5 respectively. As expected the simulation results considering the fBm model were equal to the values obtained from the buffer-dimensioning equations described in section V-A.

The results demonstrate that neither the scaling degree nor the buffer sizes impacted the PLR and the number of multiplexed video sources. For the video streams differently from the IP traffic, the buffer-size choice must consider the video sampling rates. In our analysis we consider the frame sampling rate, i.e., we expect to receive a video frame each $42ms$. Thus, considering optical link rates of 10Gbits/s and 2.5Gbits/s the buffer-size must be $\geq 424Mbit$ (see Table II). Video services delay requirements can range from $800\mu s$ (e.g., 20 Mbits/s HDTV) to $300ms$ (e.g., 64 Kbits/s videoconference) [23]. Therefore, to support video traffic with QoS requirements and the buffer pool queue size must be determined as a function of C and the service delay requirements.

The numerical results concerning the maximum number of multiplexed video sources for the optical link rates 10Gbits/s and 2.5Gbits/s are respectively summarized on Table III.

Another very important result showed that different from the scaling behavior the video traffic tail distribution strongly affected the edge-switch performance results. Nevertheless, the video distribution is a crucial point to the optical buffer dimensioning in OBS networks.

VI. CONCLUSION

In this paper we present the performance of optical switched networks to support video traffic with scaling characteristics and different QoS requirements. A new frame-to-burst (FTB) assembly was proposed to enable burst-edge-switches to support video traffic.

The $M/G/\infty$ and fBm stochastic processes were evaluated in terms of their performance to represent the video traffic scaling, heavy-tail distribution and autocorrelation. The results reported from the analysis demonstrate that the video traffic distribution can strongly influence the edge-switch buffer dimensioning and thus the optical network performance. We saw that the PLR were not affected by the the scaling degree or even the large buffer sizes. We believe that the detailed analysis presented and discussed in this paper will contribute to the design of the future optical edge-switches to deal with video traffic.

REFERENCES

- [1] P. Abry et al. Multiscale nature of network traffic. *IEEE Signal Processing Magazine*, 19(3):28–46, May 2002.
- [2] M. Barnsley et al. *The Science of Fractal Images*. Springer-Verlag New York Inc., USA, 1988.
- [3] P. Boyer and D. Tranchier. A reservation principle with applications to the atm traffic control. *Computer Network and ISDN Systems Journal*, 24:321–334, 1992.
- [4] R. Coelho and L. Decreusefond. Statistical performance of tv/hdtv traffic over broadband digital networks. *Proceedings of the IEEE GLOBECOM*, November 1998.
- [5] S. Danielsen et al. Wavelength conversion in optical packet switching. *Journal of Lightwave Technology*, 16(12):2095–2108, December 1998.
- [6] K. Dolzer and C. Gauger. On burst assembly in optical burst switching networks—a performance evaluation of just-enough-time. *Proceedings of the 17th International Teletraffic Congress*, pages 149–160, December 2001.
- [7] M. Düser and P. Bayvel. Analysis of a dynamically wavelength-routed optical burst switched network architecture. *Journal of Lightwave Technology*, 20(4):574–585, April 2002.
- [8] C. Guillemot et al. Transparent optical packet switching: The european acts keops project approach. *Journal of Lightwave Technology*, 16(12):2117–2132, December 1998.
- [9] D. Hunter and I. Andonovic. Approaches to optical internet packet switching. *IEEE Communications Magazine*, 38(9):116–122, September 2000.
- [10] E. Hurst. Long-term storage capacity of reservoirs. *American Society of Civil Engineers Trans.*, (11):770–799, April 1951.
- [11] F. Kelly. Notes on effective bandwidths. *Stochastic Networks: Theory and Applications*, 4(Oxford University Press):141–168, 1996.
- [12] M. Krusz and A. Makowski. Modeling video traffic using $m/g/\infty$ input processes: A compromise between markovian and lrd models. *IEEE J. Select. Areas Commun.*, 16(5):733–748, June 1998.
- [13] A. Law and W. Kelton. *Simulation Modeling and Analysis*. McGraw-Hill Book Company, USA, 1982.
- [14] Q. Li and D. Mills. Investigating the scaling behavior, crossover and anti-persistence of internet packet delay dynamics. *Proceedings of the IEEE GLOBECOM*, pages 1843–1852, November 2000.
- [15] B. Mandelbrot and J. Van Ness. Fractional brownian motions, fractional noises and applications. *SIAM Review*, 10(4):422–437, October 1968.
- [16] S. Molnár and A. Vidács. On modeling and shaping self-similar atm traffic. *Proceedings of the 15th International Teletraffic Congress*, pages 1409–1420, July 1991.
- [17] I. Norros. On the use of fractional brownian motion in theory of connectionless networks. *IEEE JSAC*, 13(6):953–962, August 1995.
- [18] R. Pontes and R. Coelho. The scaling characteristics of the video traffic and its impact on acceptance regions. *Proceedings of the 17th International Teletraffic Congress*, 4:197–210, December 2001.
- [19] C. Qiao et al. Optical burst switching (obs)—a new paradigm for an optical internet. *Journal of High Speed Networks*, 8(1):69–84, 1999.
- [20] M. Renaud, C. Guillemot, and B. Bostica. Network and system concepts for optical packet switching. *IEEE Communications Magazine*, (4):96–102, April 1997.
- [21] M. Roughan and D. Veith. A study of the daily variation in the self-similarity of real data traffic. *Proceedings of the 16th International Teletraffic Congress*, pages 67–76, June 1999.
- [22] M. Roughan, D. Veith, and P. Abry. Real-time estimation of the parameters of long-range dependence. *IEEE/ACM Transactions on Networking*, 8(4):467–478, August 2000.
- [23] J. Russell. *Multimedia networking performance requirements*. ATM Networks, Plenum Pubs. New York:187–198, 1993.
- [24] E. Sirén and E. Hyttiä. Delay line configurations in optical burst switching with jet protocol. Technical Report TD(02)24, COST279, May 2002.
- [25] Video Sequences Traces. Available at: *StarWars* ftp://ftp.research.telcordia.com/pub/vbr.video.trace/, *silence* and *mr_bean* http://www-tnk.ec.tu-berlin.de/fi_tzek/trace/ltvt.html, *race* http://nero.informatik.uni-wuerzburg.de/mpeg/traces/.
- [26] J. Turner. Terabit burst switching. *Journal of High Speed Networks*, 8(1):3–16, 1999.
- [27] M. Yoo and C. Qiao. Just-enough-time (jet): A high speed protocol for bursty traffic in optical networks. *Proceedings of the IEEE/LEOS Technologies for Global Information Infrastructure*, pages 26–27, August 1997.